International Journal of Pharmaceutics 379 (2009) 158–166

Contents lists available at ScienceDirect

International Journal of Pharmaceutics

journal homepage: www.elsevier.com/locate/ijpharm

Preparation and evaluation of PEG–PCL nanoparticles for local tetradrine delivery

Rutian Li[a], Xiaolin Li[b], Li Xie[a], Dan Ding[c], Yong Hu[d], Xiaoping Qian[a], Lixia Yu[a], Yitao Ding[e], Xiqun Jiang[c], Baorui Liu[a,*]

[a] The Comprehensive Cancer Center of Drum-Tower Hospital, Medical School of Nanjing University & Clinical Cancer Institute of Nanjing University, Nanjing 210008, PR China
[b] The Comprehensive Cancer Center of Drum-Tower Hospital Affiliated to Nanjing Medical University, Nanjing 210008, PR China
[c] Laboratory of Mesoscopic Chemistry and Department of Polymer Science and Engineering, College of Chemistry and Chemical Engineering, Nanjing University, Nanjing 210093, PR China
[d] National Laboratory of Solid State Microstructure, Department of Material Science and Engineering, Nanjing University, Nanjing 210093, PR China
[e] Department of Hepatobiliary Surgery, Medical School of Nanjing University, Nanjing 210093, PR China

ARTICLE INFO

Article history:
Received 25 February 2009
Received in revised form 30 April 2009
Accepted 3 June 2009
Available online 12 June 2009

Keywords:
Nanoparticles
Block copolymer
Tetradrine
Composition
HDRA

ABSTRACT

To establish a satisfactory delivery system for local delivery of Tetradrine (Tet), four kinds of core-shell nanoparticles were prepared from di-block copolymer of methoxy poly(ethylene glycol)–polycaprolactone (MePEG–PCL) and tri-block copolymer of polycaprolactone–poly(ethylene glycol)–polycaprolactone (PCL–PEG–PCL). The physiochemical traits of the four kinds of nanoparticles including morphology, particle size, zeta-potential, drug-loading content, stability, and in vitro release profile were studied. We also evaluated the four kinds of nanoparticles by in vitro cellular uptake experiment, cytotoxicity assay against LoVo cells, and biocmpatibility study. Histoculture Drug Response Assay (HDRA), a more predictive method usually used to evaluate chemosensitivity was firstly applied in our study to evaluate the antitumor potency of polymeric nanoparticles. The current study showed that all the four kinds of copolymers exhibited remarkable in vitro antitumor effects, especially in HDRA assay. The configuration and composition of the copolymers were important for the properties and functions of the nanoparticles. Nanoparticles prepared from the di-block copolymer with a particle size around 300 nm and the hydrophobic composition about 80% was determined as the most effective drug carrier for further studies.

1. Introduction

The nanoparticulate carriers developed from amphiphilic copolymers for the delivery of antitumor therapeutics have drawn intensive attention since 1990s with a lot of novel drug delivery systems developed (Pridgen et al., 2007; Gref et al., 1994; Kataoka et al., 2001; Langer, 1990). These drug carriers have the following advantages: (1) enhancing the solubility of hydrophobic agents; (2) releasing the antitumor agents in a sustainable pattern; (3) the PEG outer shell of the nanoparticles can reduce surface absorption of proteins and imparts "stealth" to nanoparticles (Pridgen et al., 2007); and (4) preferable biocompatibility and biodegradability. Therefore, a large number of block copolymers with different compositions for the delivery of chemotherapeutic agents, genes, and molecular-targeted drugs etc. have been developed and the total number is still growing (Pridgen et al., 2007). Among various copolymers, nanoparticles made of PEGylated block copolymer with good biocompatibility, such as PEGylated poly(lactide) (PLA) (He et al., 2007; Vila et al., 2005), poly(DL-glycolide-co-lactide) (PLGA) (Moffatt and Cristiano, 2006; Yang et al., 2007)and poly(caprolactone) (PCL) (Gong et al., 2008) have been widely studied and applied.

Locoregional chemotherapy is an effective treatment as much higher drug concentrations can be achieved at the site of bulk tumor and the drug induced cytotoxicity will be enhanced. (Kerr and Los, 1993; Power et al., 2008). Locoregional administration is especially important for metastatic and end-stage tumors as they are usually not able to be removed by surgical resection. The sustained-release drug delivery systems have been reported to improve the antitumor efficacy of low molecular weight agents used for local administration by overcoming the problem that free agents fail to achieve long retention in tumor tissue (Harper et al., 1999) and by attenuating local and systemic side effects (Li et al., 2008). Moreover, a recent clinical study revealed that weekly administration of RAD001, an mTORC1 inhibition, failed to treat cancers ideally because the

* Corresponding author. Tel.: +86 25 83107081; fax: +86 25 83107081.
E-mail address: baoruiliu@nju.edu.cn (B. Liu).

0378-5173/$ – see front matter © 2009 Elsevier B.V. All rights reserved.
doi:10.1016/j.ijpharm.2009.06.007

sudden blockage of mTOR pathway led to activation of MAPK pathways through feedback loops. Meanwhile, when RAD001 was treated in a low dose, high frequency pattern, the MAPK pathway was not activated (Carracedo et al., 2008). This report shed light on the prospect of sustained-release drug delivery systems in the delivery of newly developed molecular-targeted agents.

Tetradrine (Tet, Supplementary Fig. 1), a bis-benzylisoquinoline alkaloid isolated from the dried root of Hang-Fang-Chi (*Stephania tetrandra* S. Moore), is well known as its antitumor effect in vitro and in vivo. (Wang et al., 2004a). Our previous study has proved the in vivo antitumor effect of Tet by local administration (Tu et al., 2008). Despite its potential in cancer treatment, the poor water-solubility and toxicities (especially the ulcer caused by local administration, Supplementary Fig. 2) hampered further applications of Tet. To enhance the efficacy and attenuate the side effects, in this study, biodegradable amphiphilic copolymers PEGylated PCL were synthesized for local delivery of Tet.

The objectives of this study are two. First, we prepared and evaluated the antitumor effect of PEGylated PCL nanoparticles loading Tet; second, PEGylated PCL copolymers can be synthesized with different configurations (di-block copolymers and tri-block copolymers) and various compositions (different PEG/PCL ratios), which influences the properties of the copolymers and the effectiveness of nanoparticles. In order to define which composition was the fittest for the delivery of Tet, four kinds of PEGylated PCL copolymers were synthesized. The physiochemical properties, cytotoxicity and in vitro biocompatibility of the nanoparticles prepared from the four kinds of copolymers were compared. We also, for the first time, applied histoculture drug response assay (HDRA), a more predictive method evaluating chemosensitivity to evaluate the effectiveness of the nanoparticles made of different kinds of copolymers in order to define the most satisfactory one for further study.

2. Materials and methods

2.1. Materials

Tetradrine was obtained as a powder with a purity of >98% (Jiangxi Yibo Pharmaceutical Development Company, China). Methoxy-polyethyleneglycol (MePEG, M_w: 4 kDa), methoxy-polyethyleneglycol (MePEG, M_w: 2 kDa), polyethyleneglycol (PEG M_w: 6 kDa), polyethyleneglycol (PEG M_w: 10 kDa) (Sigma, USA) was dehydrated by azeotropic distillation with toluene, and then vacuum dried at 50 °C for 12 h before use. ε-Caprolactone (ε-CL, Aldrich, USA) was purified by drying over CaH_2 at room temperature and distillation under reduced pressure. Coumarin-6 (Aldrich, USA), Stannous octoate (Sigma, USA), poly(vinyl alcohol) (PVA, polymerization degree 500 and alcoholization degree 88%, Shanghai Dongcang International Trading Co. Ltd., China), RPMI 1640 (Gibco, USA), calf blood serum, (Lanzhou Minhai Bioengineering, China), and dimethylthiazoly-2,5-diphenyltetrazolium bromide (MTT, Amersco, USA) were used as received. Acetonitrile and Methanol (Merck, Germany) were of HPLC grade. All the other chemicals were of analytical grade and were used without further purification.

2.2. Synthesis of MePEG and PCL block copolymers

MePEG–PCL di-block and PCL–PEG–PCL tri-block copolymers were synthesized by a ring opening copolymerization as Zhang et al. previously described with slight modifications (Zhang et al., 2004). Briefly, predetermined amount of ε-CL was added into a polymerization tube containing MePEG or PEG and stannous octoate (0.1%, w/w). The tube was then connected to a vacuum system, sealed off, and placed in an oil bath at 130 °C for 48 h. Then the crude copolymers were dissolved with dichloromethane (DCM) and precipitated into an excess amount of cold ethyl ether to remove the un-reacted monomer and oligomer. The precipitates were then filtered and washed with water several times before thoroughly dried at reduced pressure.

A total of four kinds of block copolymers with various ratios of PEG/PCL were synthesized (two MePEG–PCL di-block copolymers and two PCL–PEG–PCL tri-block copolymers). The number-average molecular weight (M_n), weight-average molecular weight (M_w) and molecular weight distribution of these block copolymers were measured by gel permeation chromatography (GPC) (Waters 244, Milford, MA, USA) with tetrahydrofuran (THF) as the eluent at a flow rate of 1 mL/min. Calibration was accomplished using monodispersed polystyrene standards with a molecular weight range from 800 to 124,000 g/mol. The composition of the copolymers was determined by ^{1}H NMR spectra in deuterated chloroform solution, using a Bruker MSL-300 spectrometer (Faellanden, Switzerland) with tetramethylsilane as an internal standard.

2.3. Preparation of nanoparticles

Tet-loaded nanoparticles were prepared by single o/w emulsion and solvent evaporation method according to the description of Tewes et al. (2007) with modification. Briefly, 20 mg of each copolymer and a certain amount of Tet were dissolved in 1 mL of DCM. The mixture was emulsified in 3 mL of aqueous PVA solution at 5% (w/v) by sonication (XL2000, Misonix, USA) for 30 s (17.5 W) to obtain an o/w emulsion. This emulsion was then diluted in 8 mL of aqueous solution containing 1% (w/v) PVA and left under mechanical stirring for 2 h to remove DCM. The resulted solution was filtered to remove non-incorporated Tet. Blank nanoparticles were produced in the same manner without adding Tet. Finally, nanoparticle suspensions were freeze dried with 3% mannitol and stored at 4 °C.

2.4. Characterization of nanoparticles

2.4.1. Size and zeta potential analysis of the nanoparticles

Mean diameter and size distribution were measured by photon correlation spectroscopy (DLS) with a Brookheaven BI-9000AT instrument (Brookheaven Instruments Corporation, USA). Zeta potential was measured by the laser Doppler anemometry (Zeta Plus, Zeta Potential Analyzer, Brookhaven Instruments Corporation, USA). All measurements were performed at 25 °C. The values were calculated from the measurements performed at least in triplicate.

2.4.2. Morphology studies

Morphological examination of the nanoparticles was conducted using JEM-100S (Japan) transmission electron microscope (TEM). One drop of nanoparticle suspension was placed on a copper grid covered with nitrocellulose membrane and air-dried before observation.

2.4.3. Drug-loading content and encapsulation efficiency

To determine the drug-loading content, the freeze-dried powder of the nanoparticles was dissolved in acetonitrile. Tet concentration in the resulted solution was then determined by the ultraviolet absorption at the wavelength of 280 nm, a strong absorption band of Tet with reference to a calibration curve on a Shimadzu UV3100 spectrophotometer (Shimadzu, Japan). Then the total amount of the drug in the nanoparticles could be calculated.

Drug-loading content and encapsulation efficiency were obtained by the following equations:

$$\text{Drug loading content}(\%) = \frac{\text{Weight of the drug in nanoparticles}}{\text{Weight of the drug in nanoparticles} + \text{Weight of the copolymers used}} \times 100\% \quad (1)$$

$$\text{Encapsulation efficiency}(\%) = \frac{\text{Weight of the drug in nanoparticles}}{\text{Weight of the feeding drugs}} \times 100\% \quad (2)$$

2.4.4. Stability evaluation

The freeze-dried powder of the Tet-loaded nanoparticles was dissolved in purified water and then kept at room temperature. Particle sizes were determined by DLS every 3 days for 15 days to evaluate stability.

2.4.5. In vitro release of tetradrine-loaded nanoparticles

The lyophilized Tet-loaded nanoparticles were suspended in 1 mL 0.01 M phosphate buffered saline (PBS) at pH 7.4 to form the solutions containing Tet 500 μg/mL. The solution was then placed into a pre-swelled dialysis bag with a 12-kDa molecular weight cutoff (Sigma, USA) and immersed into 10 mL 0.01 M PBS of pH 7.4 at 37 °C in a constant temperature shaker. Samples were withdrawn periodically and replaced with the same amount of fresh release medium. The amount of released Tet were determined using HPLC (C18 column, Agilent Technologies, Ltd. the mobile phase consisted of methanol: water = 9:1, with 0.5% triethylamine. Flow rate of 1 mL/min, the column temperature was 25 °C, the injection volume was 20 μL, and the detector was fixed at a wavelength of 280 nm.)

2.5. Particle cellular uptake studies

The cellular uptake studies were taken according to our previous experiences. (Hu et al., 2007). LoVo cells were seeded in the 24-well plate at a density of 5×10^4 cells per well. The medium was replaced with 1 mL medium containing coumarin-6 loaded nanoparticles (12.5 μg/mL in medium) at 80% confluence for cell density. Then the plate was incubated for 0.5, 1, 2 or 4 h, the suspension was removed and each well was washed three times with PBS. Then 250 μL cell lysis solution (150 mM NaCl, 1% triton X-100, 0.1% SDS, 50 mM tris pH 8.0) was added to each well. 100 μL solution per well was transferred to a 96-well plate (black). The fluorescence intensities were determined by a microplate reader (Tecan SAFIRE, USA) with the excitation wavelength and emission wavelength 450 and 501 nm respectively. The cellular uptake efficiency was calculated as follow:

$$\text{Uptake efficiency}(\%) = \frac{I_{\text{sample}} - I_{\text{negative}}}{I_{\text{positive}} - I_{\text{negative}}} \times 100\% \quad (3)$$

I_{sample}, I_{positive} and I_{negative} are the fluorescence intensities of the sample, positive control (coumarin-6 loaded nanoparticles in cell lysis solution) and negative control (blank cell lysis solution), respectively. In these tests, each particle suspension was added to four wells for each time interval.

We also evaluated the cellular uptake of the nanoparticles qualitatively. LoVo cells were seeded onto the glass covers placed in a 6-well plate with RPMI 1640 supplemented with 10% calf serum at the density of 5×10^4 cells per well. After incubation at 37 °C in a humidified atmosphere with 5% CO_2 for 24 h, cells were exposed to medium containing coumarin-6 loaded nanoparticles (12.5 μg/mL). After incubation for 0.5, 1, 2, 4 h, each glass cover was washed 3–4 times with PBS at 4 and 37 °C respectively. Then the cells were observed under a fluorescence microscopy (Olympus BX-51, wide band Blue excitation, exciter filter BP450-480, dichroic beamsplitter DM500, barrier filter BA515).

2.6. In vitro cytotoxicity studies and biocompatibility studies

The in vitro cytotoxicity of the drugs was determined by standard MTT assays using human colon cancer cell line LoVo. Briefly, cells were seeded in a 96-well plate at a density of 5000 cells per well 24 h prior to the assay. Then cells were exposed to a series of doses of free Tet, or Tet-loaded nanoparticles. After incubation, 20 μL of 5 mg/mL MTT solution was added to each well and the plate was incubated for 4 h, allowing the viable cells to transform the yellow MTT into dark-blue formazan crystals, which were dissolved in 200 μL of dimethyl sulphoxide (DMSO). The optical density (OD) of each well was measured by an ELISA reader (ELX800 Biotek, USA) using test and reference wavelengths of 490 and 630 nm, respectively. Cell viability was determined by the following formula:

$$\text{Cell viability}(\%) = \frac{\text{OD}(\text{test well})}{\text{OD}(\text{reference well})} \times 100\% \quad (4)$$

The in vitro compatibility of the blank nanoparticles was also determined by MTT assays using LoVo and human liver cell line LO_2.

All the results obtained from MTT assays were confirmed by repeating the experiment on at least three independent occasions and testing in triplicate each time.

2.7. Histoculture Drug Response Assay (HDRA)

The HDRA was performed according to the description of Fakhrejahani et al. (2007) and Kodera et al. (2006) with slight modifications. Tissue sample was collected at surgery from a patient with gastric cancer (carida adenocarcinoma) in the Department of Gastroenterological Surgery, Drum-Tower Hospital. The experimental application of HDRA was approved by the Institutional Research Committee, and written informed consent was obtained from the patient. The fresh specimen was sampled from the primary lesion immediately after gastrectomy, stored in transportation solution (RPMI 1640 medium supplemented with 20% fetal calf serum, containing 100 IU/mL penicillin and 100 μg/mL streptomycin.) and delivered directly to the lab. The specimen was washed twice in saline, immersed in Hank's solution, and then divided into pieces of around 15 mg. The tissue was placed in a 24-well plate, into which 1-cm-square gelatin sponges had been immersed in RPMI 1640 medium supplemented with 20% fetal calf serum and amikacin sulphate 100 IU/mL containing free Tet or Tet-loaded nanoparticles at three concentrations. Four pieces of tumor specimen were incubated without any drug as control. The tissue was then cultured for 7 days at 37 °C with 5% CO_2. A mixed solution of 100 μL of 0.6 mg/ml collagenase Type I and 100 μL of 5 mg/mL MTT in 100 mg/mL sodium succinate was added. After incubation for another 24 hours, MTT-formazan was extracted by 1 mL of DMSO and 100 μl of the solution from each well was transferred to the wells of a 96-well microplate and the optical density (OD) of each well was measured by the ELISA reader using test and reference wavelengths of 490 nm and 630 nm. The viabilities of tissues were calculated according to the following formula:

$$\text{Tissue viability}(\%) = \frac{\text{OD}(\text{test})/\text{Weight}(\text{test})/\text{mg}}{\text{OD}(\text{Coontrol})/\text{Weight}(\text{Control})/\text{mg}} \times 100\% \quad (6)$$

Table 1
Chemical structure of polymers.

Sample	(nCL/nEG)[a]	(nCL/nEG)[b]	M_n[b]	M_w[c]	M_n[c]	Pd (M_w[c]/M_n[c])	Hydrophobic ratio[b]
MP-2: MePEG2K–PCL4K	0.77	0.76	5938	8060	4720	1.71	66.32%
MP-4: MePEG4K–PCL20K	1.93	1.90	23691	43763	25826	1.69	83.11%
P-6: PCL20K–PEG6K–PCL20K	2.57	2.48	44576	67368	42816	1.57	86.53%
P-10: PCL18K–PEG10K–PCL18K	1.39	1.35	44893	77634	45017	1.72	77.77%

Pd: polydispersity (defined as the ratio of weight-average molecular weight to the number-average molecular weight). *n*: number of the molecules. Hydrophobic ratio was calculated according to the following formula: hydrophobic ratio = $(M_n{}^b - M_n\,(PEG))/M_n{}^b \times 100\%$.

[a] Feeding ratio.
[b] Determined by ^{1}H NMR.
[c] Determined by GPC.

Table 2
Diameters and zeta potential of the nanoparticles.

Nanoparticles	Diameter (nm)	Polydispersity	Zeta potential (mV)
MP2	190.3 ± 1.7	0.173 ± 0.039	−0.04 ± 0.04
MP4	285.8 ± 4.2	0.054 ± 0.085	−11.47 ± 0.64
P6	333.7 ± 4.2	0.199 ± 0.043	−12.88 ± 1.65
P10	444.3 ± 7.0	0.210 ± 0.016	−7.85 ± 1.40

2.8. Statistical analysis

Statistical analyses of data were done using Student's *t* test. The data are listed as mean ± SD, and values of $P < 0.05$ were accepted as a statistically significant difference.

3. Results

3.1. Copolymer synthesis and characterization

The molecular weight of the copolymers can be obtained from ^{1}H NMR data by comparing the peak intensities of the methylene protons of the oxyethylene units of PEG to the methylene of PCL. The feeding ratio and calculated molecular weight are summarized in Table 1. The nomenclature of these copolymers was referred to the feed ratio. It was observed that calculated molecular weight was consistent with the feed ratios. As to GPC analysis, only one peak appeared in the GPC curve (data not shown), indicating that all the impurities were removed after purification. M_w and M_n were also listed in Table 1. The polydispersity of the copolymer (defined as M_w/M_n) was around 1.6. The M_n obtained from the GPC chromatogram confirmed the calculated NMR values.

3.2. Characterization of PCL–PEG nanoparticles

3.2.1. Size, zeta potential and morphology studies

The particle size and size distribution of the Tet-loaded nanoparticles in aqueous solution were determined by DLS and the results are displayed in Table 2. The particle size was presented as P10 > P6 > MP4 > MP2. Zeta potential of four kinds of nanoparticles was also listed in Table 2. All the nanoparticles are negatively charged. The particle size and zeta potential of the blank nanoparticles were not significantly different from the Tet-loaded nanoparticles (data not shown).

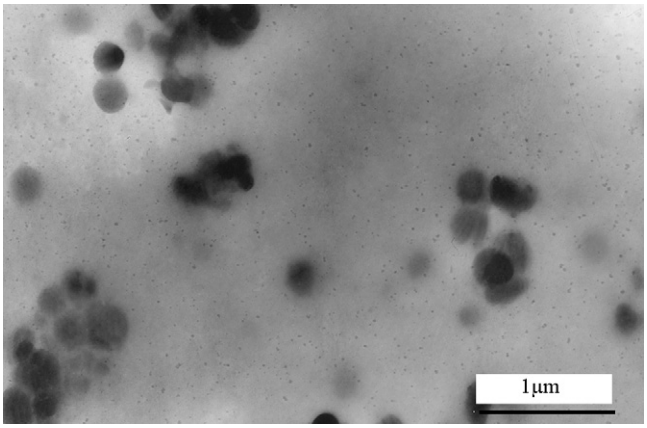

Fig. 1. TEM image of MP4 nanoparticles.

Fig. 1 presents the TEM pictures of the nanoparticles prepared by MP4. It could be observed that most of the nanoparticles exhibited a spherical shape and the size was 200–250 nm in diameter, which was in coincidence with the data from DLS (around 280 nm). So was the morphology of the nanoparticles made from the other three copolymers (figures not shown).

3.2.2. Drug-loading content and encapsulation efficiency

Table 3 listed the drug-loading content and encapsulation efficiency of each kind of nanoparticles at different Tet feedings. With the increasing of feeding, the drug-loading content increased firstly and then decreased (except for MP2). For the four kinds of nanoparticles, maximum encapsulation efficiencies were in the group with minimum feeding drug. In the following study, the feeding ratio was 10 mg/20 mg (Tet/copolymer) for MP2 and 7.5 mg/20 mg for the other three copolymers.

3.2.3. Stability evaluation

Fig. 2 shows the particle sizes' change of Tet-loaded nanoparticles within 15 days. The particle size of MP2 and P10 decreased

Table 3
The influence of drug feeding on drug-loading content and encapsulation efficiency.

Feeding ration (Tet/copolymer)	Copolymer	5 mg/20 mg	7.5 mg/20 mg	10 mg/20 mg
Drug-loading content	MP2	8.89%	10.56%	14.97%
	MP4	10.25%	14.38%	13.01%
	P6	17.25%	20.45%	16.08%
	P10	18.61%	24.60%	19.08%
Encapsulation efficiency	MP2	39.01%	31.48%	35.20%
	MP4	45.64%	44.93%	29.88%
	P6	83.38%	68.54%	38.32%
	P10	91.44%	87.02%	47.15%

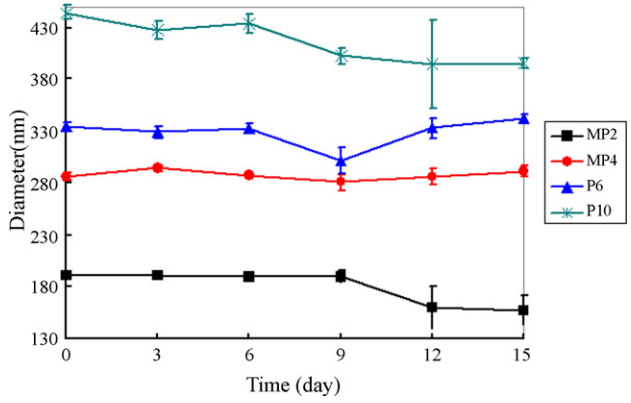

Fig. 2. Stability study of the nanoparticles. The diameter of the nanoparticles was determined by DLS and the data were presented as mean ± SD. Where bars are not shown, SD is less than the height of the points.

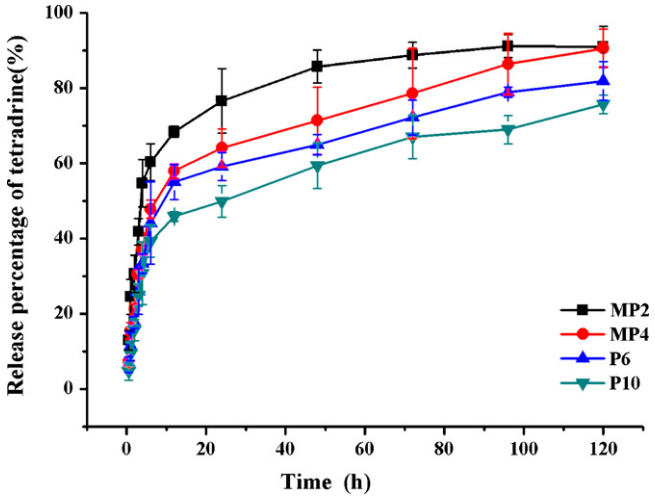

Fig. 3. In vitro release profile of Tet from the four nanoparticles. The data were presented as mean ± SD. Where bars are not shown, SD is less than the height of the points.

slightly (Day 0 vs. Day 15 190.3 ± 1.7 nm vs. 160.8 ± 14.0 nm, $P < 0.05$, 444.3 ± 7.0 nm vs. 395.3 ± 4.5 nm, $P < 0.05$, respectively.) The particles size of MP4 and P6 did not change significantly (Day 0 vs. Day 15, $P > 0.05$).

3.2.4. *In vitro release of Tet-loaded nanoparticles*

The release profiles of different Tet-loaded nanoparticles were investigated in PBS solution at 37 °C. Fig. 3 shows the cumulative in vitro release of Tet from the four kinds of nanoparticles. All nanoparticles exhibited a fast release of Tet at the initial stage and a sustained release in the following time.

MP2 presented the most prominent burst release (approximately 50% at the first 4 h and 75% at the first 24 h). The release pattern of P10 was the most sustainable with the smallest initial burst rate (approximately 30% at the first 4 h and 55% at the first 24 h.).

3.3. *Cellular uptake studies*

Particles loading fluorescent dyes are frequently used to study cellular uptake (Desai et al., 1997; Hu et al., 2007; Panyam et al., 2003). Fig. 4 shows the cellular uptake of nanoparticles with regard to different copolymers. As coumarin-6 was assumed to disperse evenly in the particles, the amount of particles was linearly proportional to the fluorescence intensities in the cells. The cellular uptake efficiency was given by the ratio between the amount of particles taken up in cells and the amount of those in the control. Time-dependent increase of uptake was observed for all nanoparticles from 0.5 to 4 h. P10 nanoparticles showed the highest uptake efficiency (12% at 4 h) while MP2 had the lowest uptake efficiency (9% at 4 h). MP4 and P6 were engulfed into cells of a similar amount.

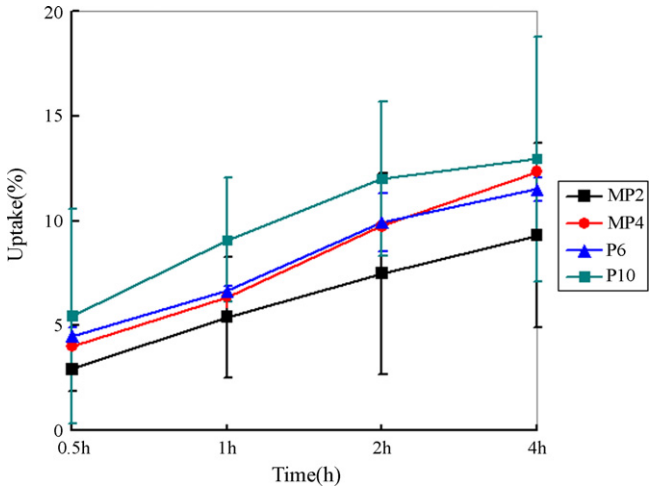

Fig. 4. The LoVo cell uptake efficiencies for different nanoparticles at different time intervals. The uptake effeicacies of the nanoparticles were presented as mean ± SD. Where bars are not shown, SD is less than the height of the points.

These results were confirmed by fluorescence microscopy observation. Fig. 5 showed the microscopic images of LoVo cells incubated with MP4 nanoparticles with 0.5, 1, 2 and 4 h at 37 °C. It can be observed that more particles were engulfed with time.

3.4. *In vitro cytotoxicity of the nanoparticles and the biocompatibility study*

Fig. 6 showed the cytotoxicity of free Tet and four kinds of Tet-loaded nanoparticles. It was observed that the cytotoxicity of Tet was positively correlated to its concentration in all the groups. The cytotoxicity of free Tet and Tet-loaded nanoparticles was similar at the concentration of 4 μg/mL. As the concentration increased, the difference of cytotoxicity between free Tet and the nanoparticles became obvious. At the concentration of 16 μg/mL, all the nanoparticles exhibited more prominent cytotoxicity than free Tet (nanoparticles vs. free Tet $P < 0.05$ at 16 μg/mL).

According to in vitro biocompatibility studies, all the blank nanoparticles exhibited little toxicity either on LO_2 cell lines (Fig. 7) or on LoVo cell lines (data not shown), which was also confirmed by the morphology of the cells observed under microscopy (Supplementary Fig. 3). The result indicated that the copolymers were nontoxic to both tumor tissue and normal tissue.

3.5. *Histoculture Drug Response Assay (HDRA)*

HDRA indicated that the antitumor effect of Tet-nanoparticles on tumor tissue was more prominent than free Tet in all nanoparticles at all tested concentrations. (Fig. 8). This difference seemed more obvious at lower concentrations. The nanoparticles made of di-block copolymers exhibited more prominent antitumor effect than those prepared from tri-block copolymers. Moreover, the antitumor effect was negatively correlated with the particle size especially at lower concentrations.

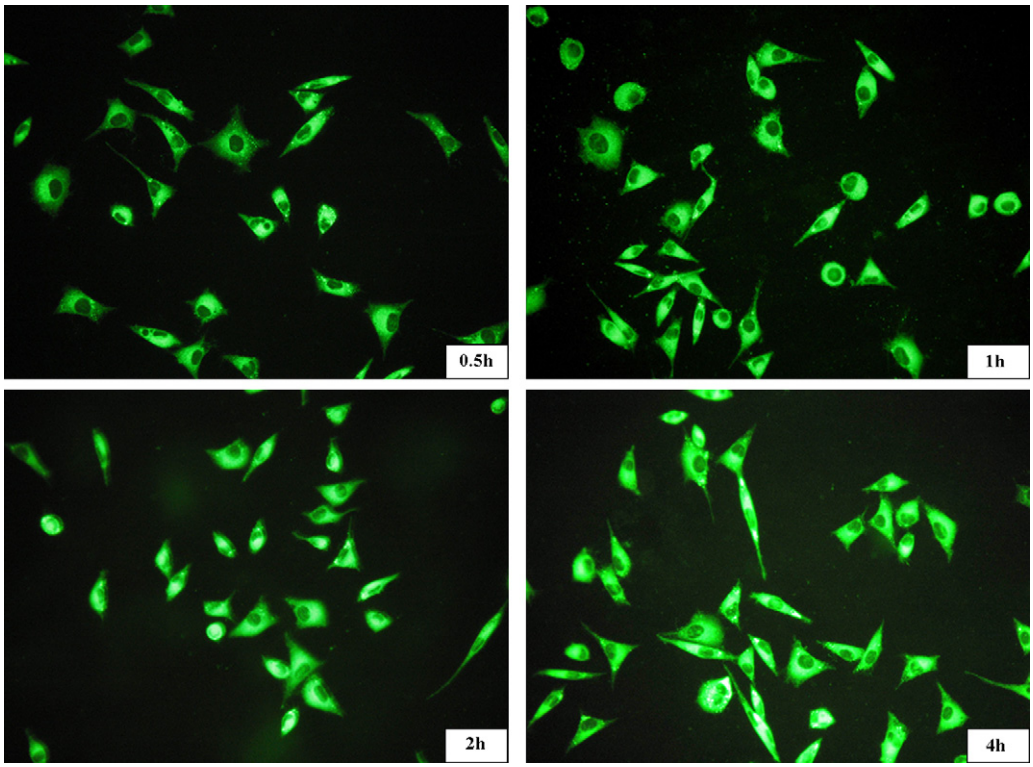

Fig. 5. Fluorescence microscopic images of LoVo cells after 0.5, 1, 2 and 4 h, incubation with different coumarin-6-loaded nanoparticles. The uptake of coumarin-6-loaded nanoparticles in LoVo cells was visualized by FITC filter (magnification = 100×).

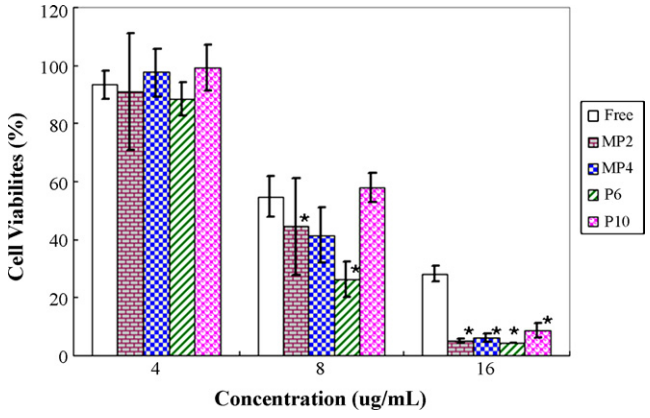

Fig. 6. The in vitro cytotoxicity of free Tet and four Tet-loaded nanoparticles to LoVo cells at different concentrations. The cytotoxicity of the nanoparticles was determined by the viabilities of cells. The data were presented as mean ± SD. *The cell viability of the nanoparticles was significantly different from those of the free Tet.

4. Discussion

In the present study we synthesized di-block copolymers and tri-block copolymers of PEGylated PCL with different PEG and PCL compositions. By evaluating their physicochemical properties and antitumor efficacy, we confirmed that the Tet-loaded nanoparticles exhibited satisfactory in vitro antitumor potency and identified MP4 as the most effective drug carrier for local administration of Tet.

Unlike systemic drug delivery, nanoparticles with larger particle size have been reported to be more effective in local delivery (Tsai et al., 2007). Therefore, we prepared the nanoparticles by the o/w emulsion and solvent evaporation method rather than the nanoprecipitation method. According to our findings, the nanoparticles prepared by the emulsion method presented significantly bigger size (200–400 nm) than those prepared by the nanoprecipitation method (less than 100 nm) (Li et al., 2008; Zhang et al., 2007). The zeta potential of MP4, P6 and P10 was around −10 mV, the absolute value of which was slightly lower than the nanoparticles prepared by the nanoprecipitation method (Hu et al., 2007; Zhang et al., 2004). As the nanoparticles prepared by emulsion method are bigger in size, the density of the neutral PEG shell is lower. Moreover, as PEG segment is uncharged and PCl segment is negatively charged, the PCL segment in the copolymers contributes to their charged state. It is obvious that the hydrophobic ratio (PCL composition) of the copolymers is in negative correlation with the absolute values of their zeta potential, which can explain why MP2 was nearly uncharged. As to the drug loading and encapsulation efficiency, maximum drug-loading content and encapsulation efficiency were observed when the feeding drug was of a suitable amount. This indicated that too much feeding drug will lead to decrease of drug-loading content by hampering the overall stability of the formed nanoparticles after Tet reached the saturation solubility in the polymer matrix (Zhang et al., 2004).

Micelles made of PEGylated PCL have been reported of preferable stability in aqueous solution (Lin et al., 2003). The nanoparticles prepared by emulsion method also exhibited good stability with no dramatic change of particle size in all the nanoparticles. The diameters of nanoparticles prepared from copolymers with lower hydrophobic ratio (MP2 and P10) decreased slightly in 15 days. This phenomenon seemed unexpected because PEG is thought to stabilize the nanoparticles. In this study, we evaluated the stability of Tet-loaded nanoparticles rather than blank nanoparticles, as Tet is a hydrophobic agent, the interaction between Tet and PCL segment may also contributed to the stability of the nanoparticles. This indicated that the hydrophobic ratio around 80% was most suitable for nanoparticles with good stability.

In the in vitro release study, P10 exhibited the most sustainable release pattern with the smallest burst release while MP2 showed the most prominent initial burst and rapid release of Tet

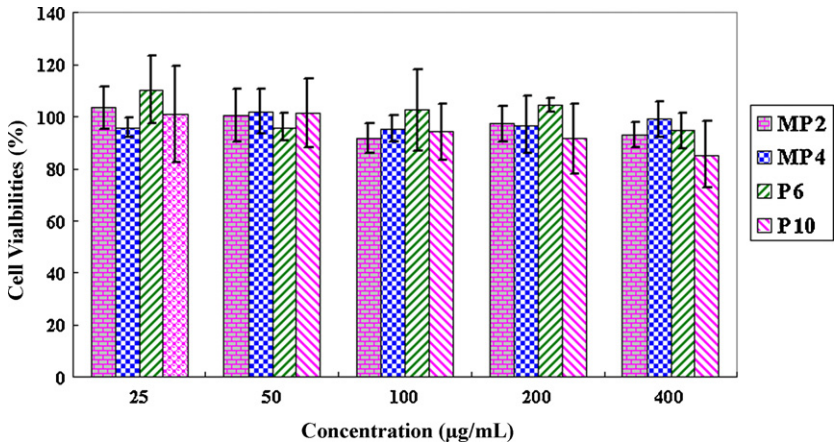

Fig. 7. The in vitro toxicity of the four blank nanoparticles at different copolymer concentrations. The cytotoxicity of the nanoparticles was determined by the viabilities of cells. The data were presented as mean ± SD.

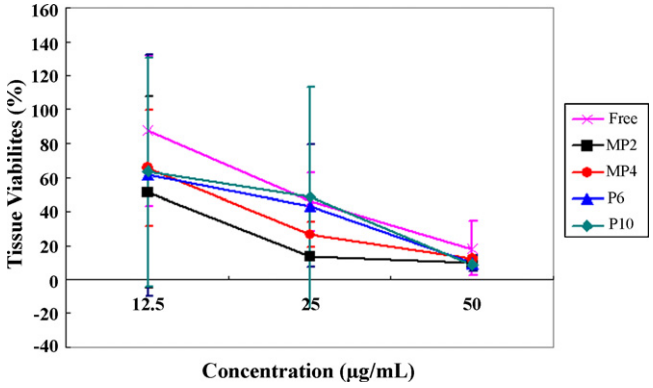

Fig. 8. Histoculture Drug Resistance Assay (HDRA) study of free Tet and Tet-loaded nanoparticles. The data were presented as mean ± SD. Where bars are not shown, SD is less than the height of the points.

(Fig. 3). All samples exhibited a fast release of Tet at the initial stage, which can be attributed to the release of Tet on the surface layers of the nanoparticles. Tet released from smaller nanoparticles more rapidly. Moreover, the nanoparticles prepared from tri-block copolymers exhibited a more sustained-release pattern. However, it was found that more Tet remained unreleased from the tri-block nanoparticles (approximately 20% for P6, 25% for P10) than that of the di-block nanoparticles (approximately 10% for MP2 and MP4) at 120 h. This may attribute to the differences between the "brush" structure for di-block copolymers and "mushroom" structure for tri-block copolymers in aqueous solution as the "mushroom" structure could form a more effective conformational cloud. (Hu et al., 2007).

The cellular uptake of the nanoparticles is also an important attribute because small molecular drugs entrapped in the nanoparticles can enter the cells through endocytosis rather than passive diffusion (Rosen and Abribat, 2005). Therefore, cellular uptake efficiency of drug-loaded nanoparticles affects the therapeutic effects. From Figs. 4 and 5, it was found that the cellular uptake of P10 nanoparticles was the most efficient at all time points while the cellular uptake proportion of MP2 was the lowest. A lot of factors have been reported to influence the uptake efficiency of nanoparticles including particle size (Zauner et al., 2001), cell lines and cell densities, hydrophobic proportion of copolymers, surface charge etc. (Foster et al., 2001; Jung et al., 2000). According to our study, particle size was found to be the main character to determine the cellular uptake efficiency. Moreover, the hydrophobic proportion of the nanoparticles also influences the uptake efficiency, as MP4 and P6 (different in particle size but similar in the hydrophobic ratio) exhibited similar uptake proportion.

As to in vitro evaluation, the cytotoxicity of both free Tet and Tet-loaded nanoparticles increased as the drug concentration grew from 4 to 16 μg/mL. The antitumor effect of the Tet-loaded nanoparticles was similar to free Tet at lower Tet concentration while the cytotoxicity of the nanoparticles was superior to free Tet at higher concentrations. This superiority may mainly due to the uptake of the nanoparticles and the sustained release of Tet inside the cancer cells. Among the four kinds of nanoparticles, it was found that P6 exhibited the most prominent cytotoxicity while P10 exhibited the mildest cytotoxicity. This difference was the most prominent at 8 μg/mL because this concentration was inside the steepest part of the dose-response curves (the inhibition rates were around 50%). The differences of cytotoxicity among the four kinds of nanoparticles can be mainly explained by the results of in vitro release and cellular uptake studies: P10 exhibited the most sustainable release pattern and only 60% Tet was released from the nanoparticles at 48 h. Moreover, Tet exhibits its effect by a variety of mechanisms including suppression of cell proliferation, promotion of apoptosis, anti-angiogenesis and reversion of drug resistance (Wang et al., 2004), so the intracellular distribution and status of Tet will influence its effectiveness. As a result, the size and conformation of the nanoparticles may also interact with Tet and indirectly affect the antitumor potency of the delivery system.

In the cytotoxicity assay, P6, MP2 and MP4 exhibited similar antitumor effect. That is because MP4 and P6 were synthesized with similar PCL composition and the two kinds of nanoparticles was similar in size. Tet released from MP2 more rapidly, but the cellular uptake of MP2 was inferior to that of P6 and MP4. As MP2 was not as stable as MP4 and P6, and the sustained-release pattern was important for the maintenance of drug at tumor site in local delivery, MP4 and P6 were hence more suitable candidates.

In order to determine which one is more preferable for Tet delivery, we evaluated the antitumor potency of the different nanoparticles using HDRA. HDRA was a technique to predict cancer patients' response to chemotherapy, which has been shown to correlate strongly with clinical outcome and survival of patients (Fakhrejahani et al., 2007). As HDRA uses tumor tissue rather than monolayer cell culture, the microenvironment and microstructure of the tumor tissue such as penetration of drug, the extracellular pH values, interstitial fluid pressure, etc. (Minchinton and Tannock, 2007) can influence the effect of drugs. As a result, the antitumor

evaluation of drugs by HDRA is expected to be more predictive than cytotoxicity assay. From this study, it is obvious that the effectiveness of the nanoparticles was superior to that of free Tet especially at lower concentrations. The superiority of the nanoparticles attributes to several reasons, firstly, Tet released in a sustained pattern from the nanoparticles, which led to longer drug retention and better effect of Tet; secondly, in the HDRA model, the drug should firstly penetrate throughout the tissue and enter the tumor cells to take effect. The nanoparticles may penetrate and taken by the cancer cells more readily compared to free Tet. Moreover, among the different nanoparticles, the results got from HDRA are not all the same as those from cell cytotoxicity assay as there are more factors affecting the antitumor effect. The penetration ability may be an important factor. Generally, small water-soluble molecules distribute most readily in the extracellular matrix, and therefore efficiently diffuse around and between cells. That is why MP2 exhibited the best effectiveness in HDRA. Also, the delivery of drugs is also determined by the drug supply; as a result, the influence of penetration tends to be more evident at lower drug concentration, which explains the more prominent differences in HDRA at lower Tet concentration. P6 in HDRA exhibited milder antitumor effect compared to MP4, which indicated that the nanoparticles prepared from di-block copolymers with PEG segment extended as a "brush" structure exhibited better penetration ability. As HDRA is more a comprehensive model than cytotoxicity assay and more rapid and convenient than in vivo evaluation, we believe that it is meaningful to apply HDRA into the evaluation of different copolymers.

Among the four copolymers, MP4 exhibited prominent antitumor effect both for in vitro cytotoxicity assay and in HDRA. Moreover, MP4 nanoparticles were proved to be of good stability and sustained-release pattern. Take all the results in this study into account, we initially choose MP4, the di-block MePEG–PCL copolymer with hydrophobic composition about 80% and M_w around 25000, as the most effective drug carrier for Tet. Obviously, this conclusion should be eventually proved in vivo, which is part of our further studies.

5. Conclusion

In the present study, core-shell structure PEGylated PCL nanoparticles was prepared from different copolymers by an emulsion method. By comprehensive evaluation, we concluded that the Tet-loaded nanoparticles showed more prominent antitumor effect than free Tet. The composition of copolymers can influence most of the properties including the antitumor effect of the drug-loaded nanoparticles. Moreover, HDRA, a model used in the evaluation of chemosensitivity, was proved to be a promising evaluation system when applied into the field of drug delivery. Nanoparticles prepared from the di-block copolymer MePEG4k-PCL20k with a particle size around 300 nm and the hydrophobic composition about 80% was determined as the most effective drug carrier for further studies.

Acknowledgements

This work was supported by the National Natural Science Foundation of China (no. 30872471), Jiangsu Province's Key Medical Center and Scientific and Technological Innovation Plan and Fund of Postgraduate from Jiangsu Province (CX08B_167Z).

Appendix A. Supplementary data

Supplementary data associated with this article can be found, in the online version, at doi:10.1016/j.ijpharm.2009.06.007.

References

Carracedo, A., Ma, L., Teruya-Feldstein, J., Rojo, F., Salmena, L., Alimonti, A., Egia, A., Sasaki, A.T., Thomas, G., Kozma, S.C., Papa, A., Nardella, C., Cantley, L.C., Baselga, J., Pandolfi, P.P., 2008. Inhibition of mTORC1 leads to MAPK pathway activation through a PI3K-dependent feedback loop in human cancer. J. Clin Invest. 118, 3065–3074.

Desai, M.P., Labhasetwar, V., Walter, E., Levy, R.J., Amidon, G.L., 1997. The mechanism of uptake of biodegradable microparticles in Caco-2 cells is size dependent. Pharm. Res. 14, 1568–1573.

Fakhrejahani, E., Miyamoto, A., Tanigawa, N., 2007. Correlation between thymidylate synthase and dihydropyrimidine dehydrogenase mRNA level and in vitro chemosensitivity to 5-fluorouracil, in relation to differentiation in gastric cancer. Cancer Chemother. Pharmacol. 60, 437–446.

Foster, K.A., Yazdanian, M., Audus, K.L., 2001. Microparticulate uptake mechanisms of in-vitro cell culture models of the respiratory epithelium. J. Pharm. Pharmacol. 53, 57–66.

Gong, C., Shi, S., Dong, P., Kan, B., Gou, M., Wang, X., Li, X., Luo, F., Zhao, X., Wei, Y., Qian, Z., 2008. Synthesis and characterization of PEG–PCL–PEG thermosensitive hydrogel. Int. J. Pharm. 365, 89–99.

Gref, R., Minamitake, Y., Peracchia, M.T., Trubetskoy, V., Torchilin, V., Langer, R., 1994. Biodegradable long-circulating polymeric nanospheres. Science 263, 1600–1603.

Harper, E., Dang, W., Lapidus, R.G., Garver, R.J., 1999. Enhanced efficacy of a novel controlled release paclitaxel formulation (PACLIMER delivery system) for local-regional therapy of lung cancer tumor nodules in mice. Clin. Cancer Res. 5, 4242–4248.

He, G., Ma, L.L., Pan, J., Venkatraman, S., 2007. ABA and BAB type triblock copolymers of PEG and PLA: a comparative study of drug release properties and "stealth" particle characteristics. Int. J. Pharm. 334, 48–55.

Hu, Y., Xie, J., Tong, Y.W., Wang, C.H., 2007. Effect of PEG conformation and particle size on the cellular uptake efficiency of nanoparticles with the HepG2 cells. J. Control. Release 118, 7–17.

Kataoka, K., Harada, A., Nagasaki, Y., 2001. Block copolymer micelles for drug delivery: design, characterization and biological significance. Adv. Drug Deliv. Rev. 47, 113–131.

Kerr, D.J., Los, G., 1993. Pharmacokinetic principles of locoregional chemotherapy. Cancer Surv. 17, 105–122.

Kodera, Y., Ito, S., Fujiwara, M., Mochizuki, Y., Ohashi, N., Ito, Y., Nakayama, G., Koike, M., Yamamura, Y., Nakao, A., 2006. In vitro chemosensitivity test to predict chemosensitivity for paclitaxel, using human gastric carcinoma tissues. Int. J. Clin. Oncol. 11, 449–453.

Langer, R., 1990. New methods of drug delivery. Science 249, 1527–1533.

Li, X., Li, R., Qian, X., Ding, Y., Tu, Y., Guo, R., Hu, Y., Jiang, X., Guo, W., Liu, B., 2008. Superior antitumor efficiency of cisplatin-loaded nanoparticles by intratumoral delivery with decreased tumor metabolism rate. Eur. J. Pharm. Biopharm. 70, 726–734.

Lin, W.J., Juang, L.W., Lin, C.C., 2003. Stability and release performance of a series of pegylated copolymeric micelles. Pharm. Res. 20, 668–673.

Minchinton, A.I., Tannock, I.F., 2007. Drug penetration in solid tumours. Nat. Rev. Cancer 6, 583–592.

Moffatt, S., Cristiano, R.J., 2006. Uptake characteristics of NGR-coupled stealth PEI/pDNA nanoparticles loaded with PLGA–PEG–PLGA tri-block copolymer for targeted delivery to human monocyte-derived dendritic cells. Int. J. Pharm. 321, 143–154.

Panyam, J., Sahoo, S.K., Prabha, S., Bargar, T., Labhasetwar, V., 2003. Fluorescence and electron microscopy probes for cellular and tissue uptake of poly(D,L-lactide-co-glycolide) nanoparticles. Int. J. Pharm. 262, 1–11.

Power, D.G., Healey-Bird, B.R., Kemeny, N.E., 2008. Regional chemotherapy for liver-limited metastatic colorectal cancer. Clin. Colorectal Cancer. 7, 247–259.

Pridgen, E.M., Langer, R., Farokhzad, O.C., 2007. Biodegradable, polymeric nanoparticle delivery systems for cancer therapy. Nanomed 2 (5), 669–680.

Rosen, H., Abribat, T., 2005. The rise and rise of drug delivery. Nat. Rev. Drug Discov. 4, 381–385.

Tewes, F., Munnier, E., Antoon, B., Ngaboni, O.L., Cohen-Jonathan, S., Marchais, H., Douziech-Eyrolles, L., Souce, M., Dubois, P., Chourpa, I., 2007. Comparative study of doxorubicin-loaded poly(lactide-co-glycolide) nanoparticles prepared by single and double emulsion methods. Eur. J. Pharm. Biopharm. 66, 488–492.

Tsai, M., Lu, Z., Wang, J., Yeh, T.K., Wientjes, M.G., Au, J.L., 2007. Effects of carrier on disposition and antitumor activity of intraperitoneal Paclitaxel. Pharm. Res. 24, 1691–1701.

Vila, A., Sanchez, A., Evora, C., Soriano, I., McCallion, O., Alonso, M.J., 2005. PLA–PEG particles as nasal protein carriers: the influence of the particle size. Int. J. Pharm. 292, 43–52.

Wang, G., Lemos, J.R., Iadecola, C., 2004. Herbal alkaloid tetrandrine: fron an ion channel blocker to inhibitor of tumor proliferation. Trends Pharmacol. Sci. 25, 120–123.

Tu, Y.X., Kong, W.W., Li, X.L., Li, R.T., Yu, L.X., Liu, B.R., 2008. Local therapeutic effect of Tetrandrine and Cisplatin on hepatocellular carcinoma in mice. Acta Univ. Med. Nanjing (Nat. Sci.) 28 (472-475), 483.

Yang, A., Yang, L., Liu, W., Li, Z., Xu, H., Yang, X., 2007. Tumor necrosis factor alpha blocking peptide loaded PEG–PLGA nanoparticles: preparation and in vitro evaluation. Int. J. Pharm. 331, 123–132.

Zauner, W., Farrow, N.A., Haines, A.M., 2001. In vitro uptake of polystyrene microspheres: effect of particle size, cell line and cell density. J. Control. Release 71, 39–51.
Zhang, L., Hu, Y., Jiang, X., Yang, C., Lu, W., Yang, Y.H., 2004. Camptothecin derivative-loaded poly(caprolactone-co-lactide)-b-PEG-b-poly(caprolactone-co-lactide) nanoparticles and their biodistribution in mice. J. Control. Release 96, 135–148.
Zhang, L., Yang, M., Wang, Q., Li, Y., Guo, R., Jiang, X., Yang, C., Liu, B., 2007. 10-Hydroxycamptothecin loaded nanoparticles: preparation and antitumor activity in mice. J. Control. Release 119, 153–162.